1H, 13C, and 15N chemical shift assignment of human PACSIN1/syndapin I SH3 domain in solution

Emmanuelle Boll, François-Xavier Cantrelle, Isabelle Landrieu, Matthieu Hirel, Davy Sinnaeve, Géraldine Levy

^{1}H, ^{13}C, and ^{15}N chemical shift assignment of Human PACSIN1/Syndapin I SH3 domain in solution

Emmanuelle Boll[ab#], Francois-Xavier Cantrelle[ab#], Isabelle Landrieu[ab], Matthieu Hirel[ab], Davy Sinnaeve[ab] & Géraldine Levy[ab**].

# contributed equally.

[a] Univ. Lille, Inserm, CHU Lille, Institut Pasteur de Lille, U1167 - RID-AGE - Risk Factors and Molecular Determinants of Aging-Related Diseases, F-59000 Lille, France.

[b] CNRS ERL Integrative Structural Biology F-59000 Lille, France.

** To whom correspondence should be addressed.

Key words: PACSIN1, SH3 domain, NMR resonance assignment, protein-protein interaction.

Biological context

The Human neurospecific PACSIN1 or Phosphoprotein Protein Kinase C and Casein Kinase substrate in neurons protein 1, which is also known as syndapin I (synaptic dynamin-associated protein), plays a central role in synaptic vesicle recycling and endocytosis, and reorganization of the microtubule and actin cytoskeleton (Modregger et al. 2002; Qualmann et al. 1999; Anggono et al. 2006). PACSIN1 comprised of 458 amino acid residues is typically found along neurites and within the synaptic boutons. In eukaryotes, PACSIN1 has two isoforms, PACSIN2 and 3, showing a wide tissue distribution (Modregger et al. 2000). PACSIN2 is ubiquitously expressed, PACSIN3 is present mainly in skeletal muscles, heart and lung, while PACSIN1 is found exclusively in the Central Nervous System (CNS). The divergence of the three isoforms spatial expression mirrors fine-tuning in their specificity in recruitment of other proteins involved in endocytosis (Modregger et al. 2000; Kessels et al. 2004). All isoforms share a highly conserved Fer-CIP4 homology-BAR (F-BAR) at its N-terminus (Qualmann et al. 2011), which consists of a 3-helix bundle and has been shown to mediate and/or stabilize membrane curvature (Rao et al. 2010; Wang et al. 2009). All PACSIN isoforms contain an SH3 domain at their C-terminus that has been shown to bind specific partners. SH3 domains bind proline-rich sequences, particularly those carrying a PxxP motif that exhibits a left-handed polyproline II (PPII) conformation (Miyoshi-Akiyama et al. 2001; Musacchio et al. 2003; Luo et al. 2016). Within the brain, the PACSIN SH3 domain has been shown to have numerous synaptic proteins as interacting partners. These include: GTPase dynamin 1 (Qualmann et al. 1999; Anggono et al. 2006), synaptojanin1 (Luo et al. 2016), synapsin1 (Kim et

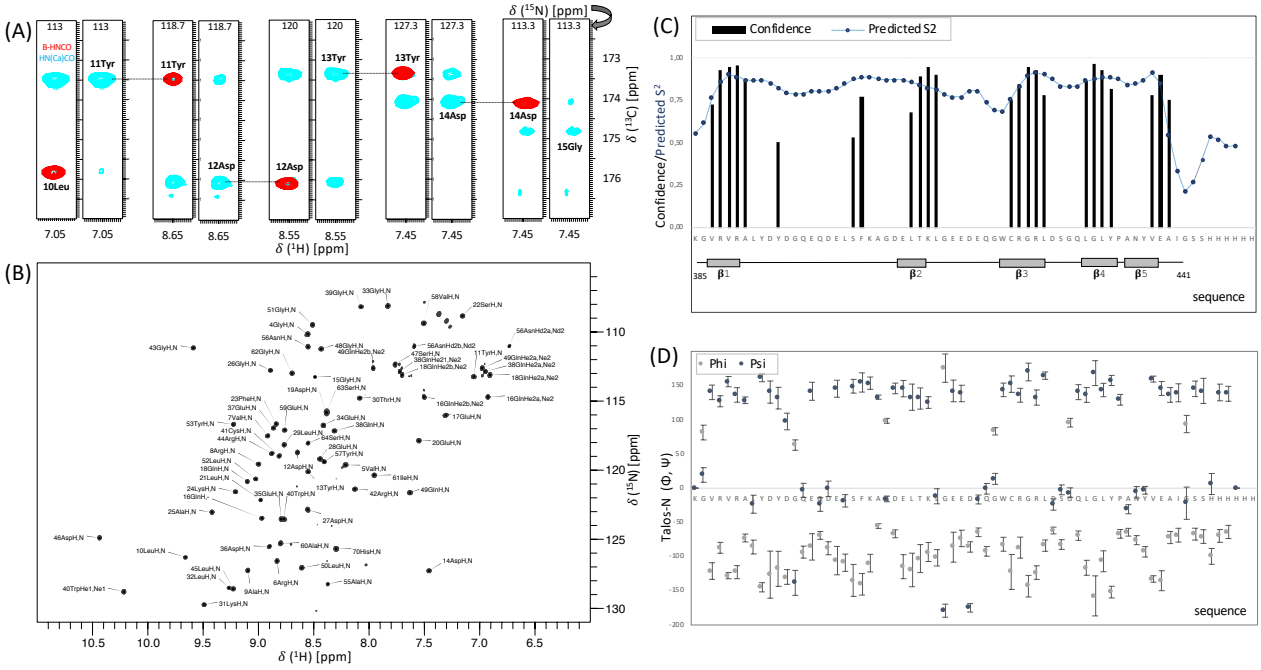

Figure 1 (A) 3D BEST-HNCO and HN(Ca)CO allow the sequential assignment of the signal detected in the HSQC spectrum of PACSIN1 SH3. Strip plots of BEST-HNCO and HN(Ca)CO spectra at the same ^{1}H and ^{15}N frequency are shown in red and cyan, respectively. The assignment resonances for residues L10 to G15 are indicated. (B) 900 MHz [^{1}H,^{15}N]-HSQC spectrum of PACSIN1 SH3 domain at neutral pH showing the resonance assignment obtained. (C) Secondary structure prediction using TALOS-N (Shen et al. 2013; Shen et al. 2015). The confidence values for regions predicted to be β-strands in black (note that no α-helixes were found in this analysis) are plotted against the sequence. Also represented in blue are the predicted order parameter (S^2) based on the chemical shifts. S^2 values closer to zero indicate higher dynamics for the given amino acid. The locations of the β-strands are shown (grey rectangles), which were obtained using a modelled structure obtained with Modeller (Sali et al. 1995) based on a sequence homology with known related structures. It took advantage of the crystal structure PDB: 2X3W, which has an 88% sequence identity with PACSIN1 SH3. (D) The ϕ (light grey line) and ψ (dark grey line) values are plotted for each amino acid. These values were predicted by TALOS-N based on the chemical shift data.

al. 2002), Tau (Liu et al. 2012), N-WASP (Fdez et al. 2007) and mSOS (Wasiak et al. 2001). Furthermore, *in vitro* and *in vivo* binding experiments demonstrated that PACSIN1 forms a complex with Huntingtin (HTT), whose pathological forms are found aggregated in Huntington Disease (HD) (Li et al. 2004). Normal functions of HTT have been the subject of intense investigations, which revealed an important role in neuronal homeostasis and survival, as it was found to be vital during early embryogenesis and development of the CNS (MacAdam et al. 2020; Liu et al. 2017). Whether the neurodegeneration observed in the adult brain is a consequence of developmental failings, or whether HTT reveals essential additional functions in the adult brain is worth further investigations. PACSIN1 was identified to form a complex including the HTT protein by binding the proline rich region in HTT, *via* its SH3 domain (Li et al. 2004; Qin et al. 2004). Interestingly the interaction is dependent on the length of HTT polyglutamine tract (Ritter et al. 1999), which is well known to modulate aggregation propensity in HTT. Also reported, is the pathological mis-localization of the PACSIN1/HTT complex in early-stage HD patients, coupled with an early impairment of PACSIN1 function (Modregger et al. 2002). This suggests a role of PACSIN1 in early neuronal evolutions seemingly through deficiency of endocytosis. Interestingly, the two other isoforms, PACSIN2 and 3 which show a wider tissue distribution including the brain, do not however interact with HTT (Modregger et al. 2002; Gao et al. 2006; Ritter et al. 1999). This is startling, as PACSIN1 and 2 differ from their isoform 3 by only two non-conservative substitutions in their 62 amino acids SH3 domain chain.

We have initiated NMR studies of the SH3 domain of Human PACSIN1 towards better understanding the interactions with the proline-rich region of HTT, aiming to elucidate the molecular basis of specificity among PACSIN SH3 domain isoforms. Here, we present ^{1}H, ^{13}C and ^{15}N assignment and chemical shifts-based predictions of the secondary structure of PACSIN1 SH3 in solution.

Methods and experiments

Expression and purification of [^{15}N]- and [^{15}N,^{13}C]-labeled SH3 of PACSIN1. The cDNA coding for Human PACSIN1 SH3 fused to a C-terminal HIS tag, was cloned into the pET 15b vector. Transformed BL-21(DE3) bacterial cells were grown in M9 medium containing ampicillin and salts with [^{15}N] ammonium chloride (1 g/l) and [^{13}C] (or [^{12}C]) glucose (2 g/l) (Cambridge Isotopes, Cambridge, MA), as sole nitrogen and carbon sources. Nickel-sepharose and Superdex 75 size-exclusion columns were successively used for protein purification prior to lyophilization. Samples for NMR measurements consisted of 300 μM protein solution in 50 mM sodium phosphate and 50 mM NaCl (pH 7.4). 10% D_2O was added for field locking, and 0.001 % TMSP for ^{1}H spectral referencing.

NMR data acquisition and processing Final volume of 330 μL were placed in 5 mm Shigemi tubes. All NMR spectra were recorded at 283 K using a Bruker AVANCE III HD 600 MHz spectrometer equipped with a CPQCI (^{1}H, ^{15}N, ^{13}C, ^{19}F) cryo-probe, or a Bruker AVANCE NEO 900 MHz spectrometer equipped with a CPTCI cryoprobe. The sequence-specific assignment was based on 2D [^{1}H,^{15}N] HSQC or HMQC, and 3D BEST-HNCO, -HNCACB, -HN(CO)CACB, -HN(CA)CO, and standard (H)CC(CO)NH, HN(CA)NNH, HN(COCA)NH, HBHANNH, HNHA, HBHA(CO)NH, H(CC)(CO)NH, HCCH-TOCSY pulse-sequences. The chemical shifts were measured relative to TMSP for ^{1}H (ν_{TMSP}). Data were transformed and processed using NMRPipe (Delaglio et al. 1995) and qMDD for acquisitions with Non-Uniform Sampling (Mayzel et al. 2014) and analyzed using CCPN analysis suite software (Vranken et al. 2005).

Extent of assignments and data deposition for PACSIN1 SH3 domain As can be seen from the strip plots of the BEST-HNCO (red) and HN(Ca)CO (cyan) in Figure 1A, the signal-to-noise of the spectra is good. This allowed for the resonance assignment detected in the [^{1}H,^{15}N]-HSQC illustrated Figure 1B, based on multidimensional NMR experiments. Backbone and side-chain sequence-specific assignment was completed at 96% for all ^{13}CO, $^{13}C_{\alpha}$ and $^{13}C_{\beta}$, 28% of $^{13}C_{\gamma\delta\varepsilon}$, and 95% of ^{1}HN and ^{15}N chemical shifts.

Secondary structure predictions and modelling

The ensemble of backbone chemical shifts ($^{13}C_{\alpha}$, $^{13}C_{\beta}$, ^{13}CO, ^{15}N and $^{1}H^{N}$) of PACSIN1 SH3 were used to estimate the secondary structures based on TALOS-N (Shen et al. 2013; Shen et al. 2015) predictions of backbone ϕ and ψ dihedral torsion angles. The analysis showed the presence of five β-strands (β_1 3-8, β_2 27-30, β_3 39-43, β_4 48-51, and β_5 56-58) predicted with high confidence, with no evidence of α-helical conformation (Fig 1C). Moreover, we used Modeller (Sali et al. 1995) to obtain a model of PACSIN1 SH3 domain based on a sequence homology with known related structures. We took advantage of the crystal structure PDB: 2X3W, which has an 88% sequence identity with PACSIN1 SH3. Comparison of the PACSIN1 SH3 domain secondary structures observed in the 3D model using ModBase (Pieper et al. 2011) with TALOS-N secondary structure predictions show good agreement (Fig 1C, bottom), with the presence of five β-strands linked by flexible loops. Moreover,

we elucidated the backbone dihedral ϕ and ψ angles on the basis of the ^{13}C shifts, Figure 1D, clearly suggesting that PACSIN1 SH3 domain is dominated by β-sheets.

A table of the assigned chemical shifts has been deposited into the Biological Magnetic Resonance Database Banks (http://www.bmrb.wisc.edu/) under the BMRB ID: 50126.

Acknowledgments

The research is supported by funding from the Métropole Européenne de Lille, through the PUSHUP project. We acknowledge LabEx (Laboratory of Excellence) for financial support on the scope of the DISTALZ consortium (ANR, ANR-11-LABX-009). The NMR facilities were funded by the Nord Region Council, CNRS, Institut Pasteur de Lille, the European Community (ERDF), the French Ministry of Research and the Université de Lille and by the CTRL CPER cofunded by the European Union with the European Regional Development Fund (ERDF), by the Hauts-de-France Regional Council (contract n°17003781), Métropole Européenne de Lille (contract n°2016_ESR_05), and French State (contract n°2017-R3-CTRL-Phase1). We acknowledge support for the NMR facilities from TGE RMN THC (CNRS, FR-3050) and FRABio (Univ. Lille, CNRS, FR-3688).

Conflict of interest

The authors declare that they have no conflict of interest.

References

Anggono V, Smillie KJ, Graham. ME, Valova VA, Cousin MA & Robinson PJ (2006) Syndapin I is the phosphorylation-regulated dynamin I partner in synaptic vesicle endocytosis. Nat. Neurosci., **9**, 752-760.

Delaglio F, Grzesiek S, Vuister GW, Zhu G, Pfeifer J & Bax A (1995) NMRPipe: A multidimensional spectral processing system based on UNIX pipes. J. Biomol. NMR, **6**, 277-293.

Fdez E & Hilfiker S (2007) Vesicle pools and synapsins: New insights into old enigmas. Brain Cell Biol., **35**, 107-115.

Gao YG, Yan XZ, Song AX, Chang YG, Gao XC, Jiang N, Zhang Q, Hu HY (2006) Structural Insights into the Specific Binding of Huntingtin Proline-Rich Region with the SH3 and WW Domains. Structure, **14**, 1755-1765.

Kessels MM. & Qualmann B (2004) The Syndapin protein family: linking membrane trafficking with the cytoskeleton. J. Cell Sci., **117**, 3077-3086.

Kim WT, Chang S, Daniell L, Cremona O, Di Paolo G & De Camilli P (2002) Delayed reentry of recycling vesicles into the fusion-competent synaptic vesicle pool in synaptojanin 1 knock-out mice. Proc. Natl. Acad. Sci., **99**, 17143-17148. Li SH & Li XJ (2004) Huntingtin-protein interactions and the pathogenesis of Huntington's disease. Trends Genet., **20**, 146-154.

Liu Y, Lv K, Li Z, Yu ACH, Chen J, Teng J (2012) PACSIN1, a Tau-interacting Protein, Regulates Axonal Elongation and Branching by facilitating Microtubule Instability. J. Biol. Chem., **287**, 39911-39924.

Liu JP & Zeitlin SO (2017) Is Huntingtin Dispensable in the Adult Brain? J. Huntingt. Dis., **6**, 1-17.

Luo L, Xue J, Kwan A. Gamsjaeger R, Wielens J, Kleist LV, Cubeddu L, Guo Z, Stow JL, Parker MW, Mackay JP, Robinson PJ (2016) The Binding of Syndapin SH3 Domain to Dynamin Proline-rich Domain Involves Short and Long Distance Elements. J. Biol. Chem., **291**, 9411-9424.

Mayzel M, Rosenlöw J, Isaksson L & Orekhov VY (2014) Time-resolved multidimensional NMR with non-uniform sampling. J. Biomol. NMR, **58**, 129-139.

McAdam RL (2020) Loss of huntingtin function slows synaptic vesicle endocytosis in striatal neurons from the httQ140/Q140 mouse model of Huntington's disease. Neurobiol. Dis., **134**, 104637.

Miyoshi-Akiyama T, Aleman LM, Smith JM, Adler CE & Mayer BJ (2001) Regulation of Cbl phosphorylation by the Abl tyrosine kinase and the Nck SH2/SH3 adaptor. Oncogene, **20**, 4058-4069.

Modregger J, Ritter B, Witter B, Paulsson M & Plomann M (2000) All three PACSIN isoforms bind to endocytic proteins and inhibit endocytosis. J. Cell Sci., **113**, 4511-4521.

Modregger J, DiProspero NA, Charles V, Tagle DA & Plomann M (2002) PACSIN1 interacts with huntingtin and is absent from synaptic varicosities in presymptomatic Huntigton's disease brains. Hum. Mol. Genet., **11**, 2547-2558.

Musacchio A & Wodak SJ (2003) How SH3 Domains Recognize Proline. Adv. Protein Chem., **61**, 211-268.

Qin ZH, Wang Y, Sapp E, Cuiffo B, Wanker E, Hayden MR, Kegel KB, Aronin N & diFiglia M (2004) Huntingtin bodies sequester vesicle-associated proteins by a polyproline-dependent interaction. J. Neurosci., **24**, 269-281.

Qualmann B, Roos J, DiGregorio P J & Kelly RB (1999) Syndapin I, a Synaptic Dynamin binding Protein that Associates with the Neural Wiskott-Aldrich Syndrome Protein. Mol. Biol. Cell., **10**, 501-513.

Qualmann B, Koch D & Kessels MM (2011) Let's go bananas: revisiting the endocytic BAR code. EMBO J., **30**, 3501-3515.

Pieper U, Webb BM, Barkan DT, Schneidman-Duhovny D, Schlessinger A, Braberg H, Yang Z, Meng EC, Pettersen EF, Huang CC, Datta RS, Sampathkumar P, Madhusudhan MS, Sjolander K, Ferrin TE, Burley SK, Sali A (2011) ModBase, a database of annotated comparative protein structure models, and associated resources. Nucleic Acids Research, **39**, 465-474.

Rao Y, Ma Q, Vahedi-Faridi A, Sundborger A, Pechstein A, Puchkov D, Luo L, Shupliakov O, Saenger W & Haucke V (2010) Molecular basis for SH3 domain regulation of F-bar-mediated membrane deformation. Proc. Natl. Acad. Sci., **107**, 8213-8218.

Ritter B, Modregger J, Paulsson M, Plomann M, (1999) PACSIN2, a novel member of the PACSIN family of cytoplasmic adapter proteins. FEBS Lett., **454**, 356-362.

Šali A, Potterton L, Yuan F, Vlijmen H van & Karplus M (1995) Evaluation of Comparative Protein Modelling by MODELLER. Proteins Struct. Funct. Bioinforma., **23**, 318-326.

Shen Y & Bax A (2013) Protein backbone and sidechain torsion angles predicted from NMR chemical shifts using artificial neural networks. J. Biomol. NMR, **56,** 227-241.

Shen Y & Bax A (2015) Protein Structural Information Derived from NMR Chemical Shift with the Neural Network Program TALOS-N. Methods Mol. Biol., **1260**, 17-32.

Vranken WF, Boucher W, Stevens TJ, Fogh RH, Pajon A, Llinas M, Ulrich EL, Markley JL, Ionides J, Laue ED (2005) The CCPN data model for NMR spectroscopy: development of a software pipeline. Proteins, **59**, 687-696.

Wang Q, Navarro MVAS, Peng G, Molinelli E, Goh SL, Judson BL, Rajashankar KR, Sondermann H (2009) Molecular mechanism of membrane constriction and tabulation mediated by the F-BAR protein PACSIN/Syndapin. Proc. Natl. Acad. Sci. U. S. A., **106,** 12700-12705.

Wasiak S, Quinn CC, Ritter B, de Heuvel E, Baranes D, Plomann M & McPherson PS (2001) The Ras/Rac Guanine Nucleotide Exchange Factor Mammalian Son-of-sevenless Interacts with PACSIN1/Syndapin I, a Regulator of Endocytosis and the Actin Cytoskeleton. J. Biol. Chem., **276**, 26622-26628.